Catena 261 (2025) 109559

Contents lists available at ScienceDirect

Catena

journal homepage: www.elsevier.com/locate/catena

# Resilience of mangroves to climate and land-use changes in the Pacific Islands☆

Eliana Jorquera [a], José F. Rodríguez [a,*], Patricia M. Saco [a,b], Steven Sandi [c], Juan Quijano-Baron [a], Angelo Breda [a,d]

[a] School of Engineering, University of Newcastle, Callaghan 2308, Australia
[b] School of Civil and Environmental Engineering, University of Technology Sydney, Sydney, Australia
[c] School of Civil and Environmental Engineering, Deakin University, Geelong, Australia
[d] Water Modelling Systems, WaterNSW, Sydney, Australia

ARTICLE INFO

*Keywords:*
Ecogeomorphological modelling
Coevolution
Sedimentation
Climate change
Land use change

ABSTRACT

Mangrove wetlands in Pacific Islands are vital ecosystems that provide important services such as habitat for marine species, flood protection and carbon storage. They occupy low-lying areas that are at risk of sea level rise (SLR), which, combined with anthropogenic pressures exerted on adjacent zones can lead to destabilising effects on these ecosystems. Their resilience to climate and land use changes is closely related to sediment availability, as mangroves can vertically adjust their soil surface (accretion) by trapping sediment and building root mass, offsetting SLR. In this contribution, an ecogeomorphological model is applied to a mangrove wetland site in Vanua Levu Island, Fiji, to predict its evolution over the next 100 years and to assess its resilience under five different scenarios of climate and land use change. Scenarios consider the SSP5-8.5 pathway SLR and include a scenario with current conditions, two scenarios with different levels of deforestation in the catchment, one scenario with increases in temperature and rainfall intensity, and a scenario with conservation practices to reduce sediment from the catchment. Changes in the catchment are assessed using a hydro-sedimentological model previously calibrated, and produce increases in sediment supply to the wetland for all scenarios except the conservation scenario. Changes in sediment supply are incorporated into the ecogeomorphological model, which is able to quantify improvements in the resilience of the wetland due to increases in sediment. Improvements in resilience are not enough to prevent substantial wetland losses (30 % to 60 %) because mangroves cannot colonise new areas due to topographic constraints and a manmade embankment that prevents tidal incursion. The methodology uses numerical models that are set up and verified with regional information and remote sensing derived data, so it has enormous potential for the assessment of wetland vulnerability in other mangrove wetlands of the world with limited ground information.

## 1. Introduction

Mangrove wetlands are vital ecosystems that provide important services such as nursery habitat for marine species, flood regulation, and carbon storage, among others (Beck et al., 2001; Kelleway et al., 2017; Ludwig et al., 2019; Sandi et al., 2021). They are located in low-lying areas that are at risk of sea level rise (SLR), which, combined with anthropogenic pressures exerted on adjacent zones can lead to destabilising the fragile balance of all factors that compound these ecosystems.

Research has shown that the resilience of mangrove wetlands to SLR is closely related to sediment availability. Wetlands are depositional environments and mangroves can vertically adjust the surface of the forest floor by trapping sediment and building root mass (Saintilan et al., 2020; Krauss et al., 2014; Lovelock et al., 2015; Hayden and Granek, 2015; van Maanen et al., 2015). This adjustment (known as biogeomorphic accretion) can help mangroves keep up with SLR under particular conditions of suspended sediment and tidal levels, as shown by several studies using both field and numerical modelling results (Hayden and Granek, 2015; Krauss et al., 2014; Lovelock et al., 2015;

☆ This article is part of a special issue entitled: 'landscape (co)evolution' published in Catena.

* Corresponding author.
*E-mail address:* jose.rodriguez@newcastle.edu.au (J.F. Rodríguez).

https://doi.org/10.1016/j.catena.2025.109559
Received 15 June 2024; Received in revised form 30 September 2025; Accepted 13 October 2025
Available online 24 October 2025

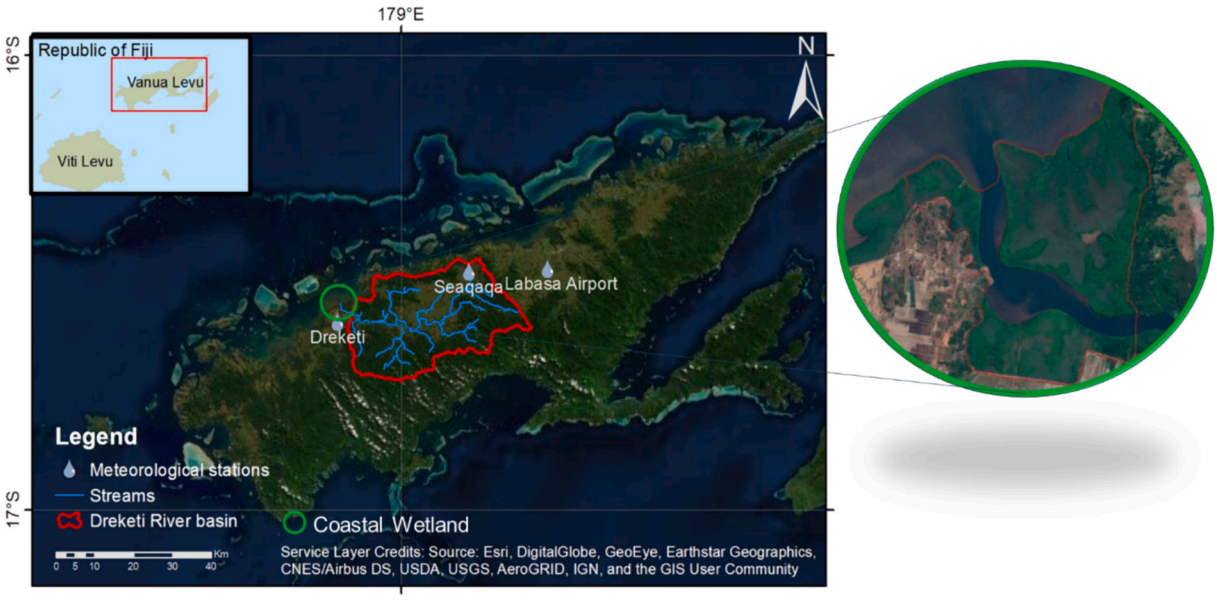


**Fig. 1.** Geographic location of Dreketi River catchment and its wetland.

Rodriguez et al., 2017; Sandi et al., 2018; van Maanen et al., 2015; Breda et al., 2022). The availability of sediment can also be influenced by land use practices in the catchment, as different land uses are associated with different levels of sediment production. Deforestation and transformation into agricultural land is typically associated with increases in sediment production, which may be reflected in increases in sediment availability in the wetland areas.

Modelling the evolution of mangrove wetlands considering accretion and sea level rise is challenging due to the complexity of the processes co-evolving at a variety of spatial and temporal scales. Mangrove wetlands respond to SLR via accretion but also via landward migration. These two processes operate at relatively long scales (several years) but they integrate a number of other processes that occur at smaller scales. Accretion is a function of the tidal regime, sediment availability and type of vegetation (Fagherazzi et al., 2012; Lovelock et al., 2015). The resilience of the vegetation is heavily influenced by the complex interaction between plant biological processes, frequency of floods and sediment inputs (Cahoon et al., 2021; Woodroffe et al., 2016). As such, the combination of flood characteristics (hydroperiod, tidal range, etc) and environmental conditions (salinity, soil type, etc) drive the survival and establishment of vegetation in newly colonized areas (Crase et al., 2013; Krauss et al., 2008). In order to be able to model wetland evolution under SLR, current models have to reach a compromise between reasonable computational running times and a model complexity that ensures that the most relevant processes are considered. A good balance has been achieved by eco-geomorphological models that integrate detailed simulations of tidal and sediment dynamics over a short period (several tidal cycles representing the annual variation) that can be used to determine yearly vegetation distribution and accretion values, with longer term multi-year geomorphological simulations with updates of the domain (topography and vegetation) and input conditions (including tidal changes due to SLR) at the end of that period to continue the calculations of these coevolving system for successive periods (Rodriguez et al., 2017; Sandi et al., 2018; Breda et al., 2021).

One of the challenges of predicting wetland evolution using process-based models is the availability of reliable data for model setup and verification. This is an important consideration for a modelling strategy, particularly in remote areas with very limited ground information. Remote sensing data can be used at different stages of the modelling, but requires additional tests to verify the validity of data and results. Using predominantly remote sensing data also means that the methodology has enormous potential for the assessment of wetland vulnerability in other mangrove wetlands of the world with limited ground information.

Historically in Fiji, mangroves have been one of the primary sources of natural resources, providing food and fuel to the surrounding communities (Ash, 1992). The Republic of Fiji has more than 380 km$^2$ covered by mangrove wetlands, ranking as the third nation among the Pacific Island Countries in mangrove coverage, after Papua New Guinea and the Solomon Islands (SPREP, 2016). Islands of the tropics have been identified as hotspots for climate change impacts (IPCC, 2021), and the effects of climate change are expected to be quite severe in the low-lying coastal areas of the Pacific Islands due to the combination of SLR and extreme weather. Extreme events are characterised by intense precipitation, which generates flooding and sediment exports from catchments into the coastal areas (Terry et al., 2004; McInnes et al., 2014; Magee et al., 2016, Kostaschuk et al., 2001). In addition, severe storm events such as hurricanes and cyclones can have diverse effects on mangroves, while in some cases sediment inputs can contribute to maintaining elevation under sea level rise (Cherry and Battaglia 2019; Feher et al., 2020), some extreme events may lead to a complete collapse of the vegetation and transition to mudflats (Osland et al., 2020). Among catchments draining their waters onto the coast, the rural catchment of the Dreketi River in the Vanua Levu Island of Fiji stands out due to its significant sediment contribution (Brown et al., 2017) and also because it has a mangrove wetland that is part of the Qoloqoli Cokovata, a RAMSAR site since 2018 (Ramsar Convention Secretariat, 2019). In addition, catchments in this area have experienced land use changes in the past involving deforestation for logging, and for urban and agricultural repurposing of the land, with sugar cane plantations constituting the main industrial crop in the Dreketi catchment. Further changes in land use can have significant implications for coastal ecosystems, particularly when combined with SLR.

In this contribution an ecogeomorphological model is applied to a mangrove wetland in the Dreketi river to predict its evolution and to assess the resilience of the wetland to climate and land use change. The main novelty of our contribution consists of the coupling of the wetland ecogeomorphological model to a catchment hydro-sedimentological model (see Jorquera et al., 2024 and Supplementary Material) to determine catchment sediment exports under several scenarios that combine climate change and land use changes. We hypothesize that these changes can pose a significant threat to mangrove ecosystems in the Dreketi catchment. The importance of this ecosystem and the

potential vulnerability to future conditions justifies its selection as a study site representative of the mangrove wetlands in Fiji and their future evolution.

## 2. Methods

### 2.1. Study site

In Fiji, wetland habitats can be classified in four major categories: *Rhizophora* forest, *Brugeria* forest, mixed mangrove forest and species growing on the landward edge of the mangrove forest (SPREP, 2016). However, there is a lack of information regarding the characteristics of the wetlands in terms of extension, the health of the vegetation and details of the species distribution (SPREP, 2017). The mangrove wetland at the mouth of the Dreketi River has an area of approximately 6.8 $km^2$, including the area occupied by the river and the channels (Fig. 1). The characteristics of the wetland are similar to one of the communities described for the Labasa wetland (Scott, 1993). The main species are *Rhizophora Samoensis, Bruguiera gymnorrhiza* and the hybrid *Rhizophora* × *selala.* According to Scott (1993), *Rhizophora Samoensis* dominates the area at the back of the river banks, the seaward edge and the hypersaline mudflats, whereas *Bruguiera gymnorrhiza* and the hybrid *Rhizophora* × *selala* are increasingly more frequent towards the outer edge.

### 2.2. Eco-geomorphological model

The modelling framework used in this contribution was implemented by Rodriguez et al. (2017); Sandi et al. (2018) and Breda et al. (2021). The framework is spatially distributed over a regular structured grid and combines hydrodynamic, vegetation and sedimentation/accretion models that can simulate the co-evolution of these important processes over long time scales.

The hydrodynamic model calculates the distribution of water levels and velocities over the simulation domain using a scheme of cells developed by Riccardi (2000). The model solves the simplified Saint-Venant equations of mass and momentum for shallow water on a rectangular cell-grid. The conservation of mass for each cell is expressed in the model as:

$$S_i \frac{dz_i}{dt} = \sum_{k=1}^{j} Q_{k,i} \tag{1}$$

where $S_i$ is the surface area of cell $i$, $z_i$ is the water surface elevation, $Q_{k,i}$ is the flow between cell $i$ and $k$, given that cell $i$ has $j$ neighbouring cells. There are two types of cells: channel or land. Therefore, there are three types of links: land-land, channel-channel and land-channel. The discharge between cells is based on the conservation of energy equation and is computed from the water surface gradient ($z_k - z_i$). In land-land as an example, where there is a preponderance of gravity, hydrostatic pressure and friction forces, the discharge is given by:

$$Q_{k,i} = sign(z_k - z_i)\frac{A_{k,i}R_{k,i}^{2/3}}{n_{k,i}}\sqrt{\frac{|z_k - z_i|}{\Delta x_{k,i}}} \tag{2}$$

where $A_{k,i}$, $R_{k,i}$ and $n_{k,i}$ are, respectively, the wetted area, hydraulic radius, and the Manning roughness coefficient in the interface between cells $i$ and $k$. The last is given by the average value between the coefficients of each cell. The variable $\Delta x_{k,i}$ is the distance between the centres of the cells. Slightly different formulations are used for the other kinds of links, but they are also based on the energy equation. The system of equations is numerically solved using a Gauss-Seidel iteration method (Riccardi, 2000), and the parameters of the model are the roughness coefficient for the land and channel cells.

The hydrodynamic model allows the calculation of the average depth of water below mean high tide (D) and the percentage of time in a year that the cell is inundated (denominated as hydroperiod, H). Those two characteristics summarise the driving factors for vegetation establishment and growth, and they are applied through a series of vegetation establishment/survival rules specific for a vegetation type (D'Alpaos et al., 2007; Lovelock et al., 2015; Saco and Rodríguez, 2013). The values for establishment/survival for mangroves (see Section 3.2) are compared with the H and D values estimated from the water levels calculated by the hydrodynamic model, and if hydrodynamic conditions produce values above the establishment/survival threshold the vegetation is present in the cell.

**Table 1**
Parameters for soil elevation model and above biomass equation.

| Model parameter | Value | Source |
|---|---|---|
| $q$($m^3$ $year^{-1}$) | $9.0 \times 10^{-5}$ | Rodriguez et al., 2017 |
| $k$($m^5$ $g^{-2}$ $year^{-1}$) | $1.3 \times 10^{-7}$ | Rodriguez et al., 2017 |
| $a$(g $m^{-3}$) | −42,037 | Kauffman et al., 2011 |
| $b$(g $m^{-4}$) | –5827.9 | Kauffman et al., 2011 |
| $c$(g $m^{-2}$) | 41841.0 | Kauffman et al., 2011 |

The vegetation feedback in the modelling framework is related to changes in surface roughness and accretion rates. Roughness will affect the hydrodynamic model flow resistance, and accretion (calculated through the geomorphological module) will change the domain topography. Accretion considers that mangroves trap sediments and transfer biomass to the soil, increasing the soil surface elevation. This process is known as bio-geomorphic accretion and is calculated following Morris et al. (2002) equation as adapted by Rodriguez et al. (2017):

$$\frac{dE}{dt} = C(q + kB)D \tag{3}$$

where $E$ stands for surface elevation, $C$ is the suspended sediment concentration, $B$ is the above ground biomass and $q$ is a depositional parameter. This model considers two main drivers of soil elevation: the deposition of suspended solids, controlled by the sedimentation rate $q$, and sediment trapping and biomass transfer by vegetation, controlled by a trapping efficiency coefficient $k$. The values of these parameters ($q$ and $k$) are a function of the vegetation and the sediment material. Table 1 presents the parameters used to model the bio-geomorphic accretion, which were obtained from Rodriguez et al. (2017) for mangrove species in muddy substrates. The values of $q$ and $k$ adopted by Rodriguez et al. (2017) correspond to a different species of mangrove (Avicennia marina), so they have been used as an approximation in the absence of local information. However, Rodriguez et al. (2017) indicated that $q$ depends on sediment type only and successfully applied a value of $q$ reported by Morris et al. (2002) for a similar sediment type (mud) and adjusted $k$ (dependent on vegetation type) so that Eq. (3) would result in a value of accretion rate compatible with the measured accretion rate. The same rationale was applied here, and the value of k proposed by Rodriguez et al. (2017) did not required adjustments as the predicted accretion rates matched values reported in the literature (see Section 3.2.1). The above-ground biomass is calculated in cells where mangrove is present using:

$$B = aD + bD^2 + c \tag{4}$$

where $a$, $b$, and $c$, are empirical coefficients that depend on the vegetation characteristics and obtained from Kauffman et al. (2011) for similar mangrove species in Micronesia. Eq. (4) has been developed for saltmarsh (Morris et al., 2002) and extended to mangroves (Rodriguez et al., 2017; Sandi et al., 2021; Morris et al., 2023). It not only provides a spatial distribution of above-ground biomass but also allows for a dynamic update of biomass if D changes during the simulation period.

The values of sediment concentration C in Eq. (3) are obtained using the catchment inputs and a transport model for very fine sediment (mud)

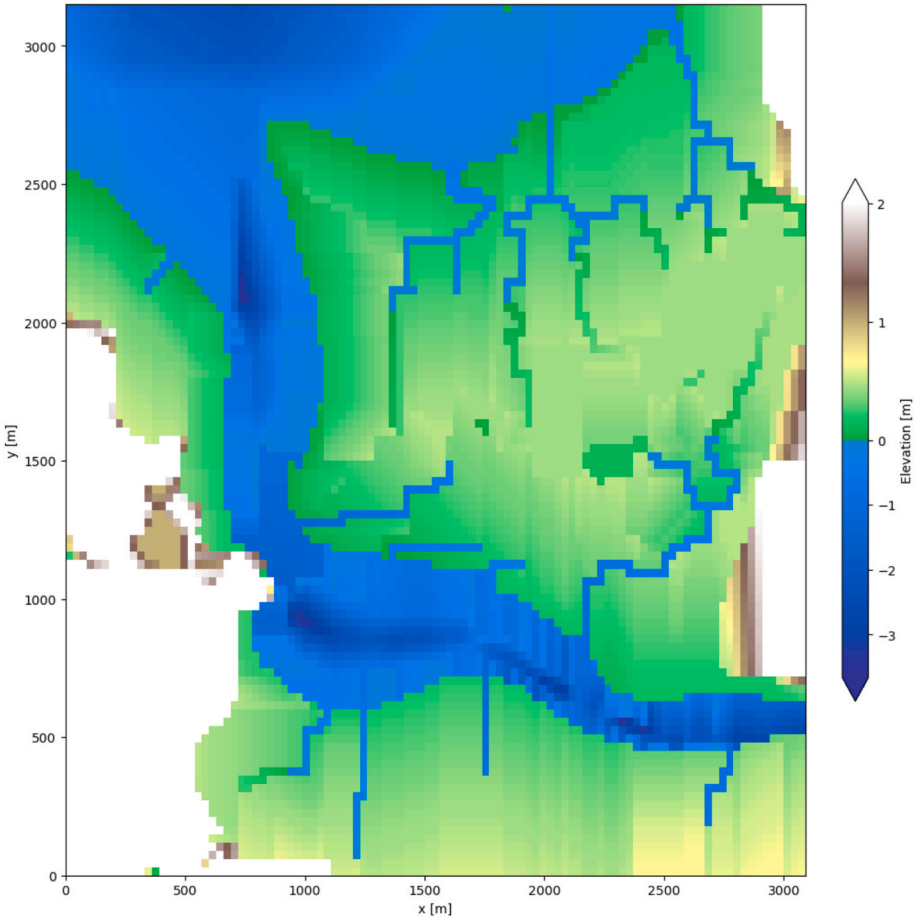


**Fig. 2.** Representation of the topography of the Dreketi mangrove wetland.

developed by Breda et al. (2021).

### 2.3. Model set-up and parameterisation

The first step in the model set-up is the definition of the topography of the wetland and the adjacent area. A DEM from the Advanced Spaceborne Thermal Emission and Reflection Radiometer of Global DEM (ASTER GDEM) (https://lpdaac.usgs.gov) with spatial resolution of one arc-second (30 m × 30 m) was used for the Dreketi wetland. The DEM was adjusted to account for potential errors in elevation induced by the presence of wetland vegetation in low relief areas by subtracting the estimated vegetation height to the original DEM data. The vegetation height was estimated from site descriptions (Scott, 1993) and from comparison of elevations at adjacent DEM grid points with and without vegetation as identified by supervised classification of Landsat images. For the mouth of the river and the main channel we complemented the DEM with historical navigation charts that contained detailed elevation. These charts were retrieved from https://data.linz.govt.nz/ and digitised. Fig. 2 presents the topography used for eco-geomorphological modelling purposes.

The hydrodynamics of the wetland are driven by the tidal regime, but detailed hourly data of tidal levels were not available in the area. A simplified sinusoidal tidal regime representing mean tide conditions, with an amplitude of 1.5 m and period of 12 h was used for simulation purposes, as done in previous research (Kirwan et al., 2010, 2013, 2016; Breda et al., 2021; D'Alpaos et al., 2007). This tidal regime was derived from local predictions of high and low tide for the area (https://tidechecker.com/fiji/northern-division/dreketi/).

The simulation domain was defined as a grid of 10,815 cells arranged in a rectangular area 3090 m wide by 3150 m long. The dimension of the cells was determined by the DEM resolution of 30 m. There are two types of cells, channel and overland. Also included in the domain is an embankment and a channel that were built over 40 years ago to drain the south part of the wetland and convert it to agricultural land (Ash, 1992). The hydrodynamic model was setup with a value of Manning roughness coefficient n (Eq. (2)) of 0.5 for mangrove areas and of 0.12 for unvegetated substrates following Rodriguez et al. (2017); Knight (1981); Mazda et al. (1997), and Dietrich et al. (2011).

An average sediment concentration of 40 mg/L was used for current conditions based on results of a hydro-sedimentological model applied to the contributing catchment (Jorquera et al., 2024), which is in line with other estimates in the area (Brown et al., 2017).

The model considers that the tidal regime defines the vegetation establishment and survival. The depth below mean high tide, D, and the hydroperiod H computed on every cell were used to characterise the tidal regime (Breda et al., 2021). Suitable conditions for vegetation establishment will depend on the mangrove species (Crase et al., 2013). The suggested values for H and D, documented in previous works in Indo-Pacific mangroves wetlands that are similar to *Rhizophora*, are H lower than or equal to 50 %, and D greater than 12 cm (Rodriguez et al., 2017; Crasse et al., 2013). In the absence of information on the distribution of mangrove species in the wetland, the same condition was applied to all the mangrove species present in the wetland. This is supported by observations that *Rhizophora samoensis* and *Bruguiera gymnorrhiza* have the same preference to tidal conditions and their zonation responds to chemical dispersal, competitive ability, and susceptibity to herbivory (Smith, 1987), It is also very likely that *Rhizophora selala* has the same preference as it is a hybrid of *Rhizophora samoensis*. Freshwater vegetation is assumed in areas not exposed to saltwater (H = 0 %, D~0 m). Table 1 presents the parameters used for

**Table 2**
Scenarios for resilience analysis.

| Scenarios | Sediment change | Sediment input (mg/L) | Comments |
|---|---|---|---|
| Baseline | – | 40 | Sediment concentration for current conditions and SLR |
| RA-I | +10 % | 44 | Sediment concentration increase from changes in land use (5 %) and SLR. |
| RA-II | +30 % | 52 | Sediment concentration increase from changes in land use (10 %) and SLR |
| RA-III | 0–60 % | 40–64 | Sediment concentration increase for changes in rainfall intensity and SLR |
| RA-IV | −30 % | 28 | Sediment decreases and SLR |

the mangrove species in the soil elevation model (Eq. (3)), and the calculation of above ground biomass (Eq. (4)).

Because of the lack of data for model calibration, the vegetation model (without any updates from eco-geomorphological feedbacks) was run for one year under current conditions and the results were compared with the observed vegetation distribution in order to test that the setup and model parameters were suitable for the simulation of the Dreketi wetland. In the same way, the eco-geomorphological model results for current conditions were tested by comparing computed accretion with estimates of accretion based on observations (see 3.1).

### 2.4. Resilience analysis scenarios

The eco-geomorphological model was applied to the Dreketi mangrove wetland to assess its resilience under future conditions. As mentioned, one of the primary inputs of the model is sediment concentration. We studied four future scenarios, named resilience analysis I to IV (RA I to IV) and a baseline case.

To assess the resilience of the Dreketi mangrove wetland, the response of vegetation dynamics and the accretion rates were evaluated under possible future scenarios over 100 years (Text S1 in Supplementary Material). First, the sediment exports from the Dreketi River catchment were calculated for future scenarios of land use changes and climate change using the same hydro-sedimentological model calibrated for the contributing catchment (Jorquera et al., 2024). Afterwards, the eco-geomorphological model was applied using the sediments estimated from the catchment simulations jointly with the projections of SLR. We explored five different scenarios to assess the mangrove wetland resilience (Table 2). The rate of SLR was the same for all the scenarios, corresponding to the lower limit of the SSP5-8.5 projections with a total rise in sea level of 700 mm in 100 years (IPCC, 2021). The baseline scenario considered the current sediment inputs and projected SLR. Scenarios for Resilience Analysis (RA) I and II represented increases in sediment (10 % and 30 %, respectively) due to changes in land use and cover associated with expansion of agriculture in the catchment (Text S2, Figs. S2 and S3). For the RA I scenario we considered that agriculture replaces all other land uses in areas with a terrain slope of 5 % or less, whereas for the RA II that limit of the terrain slope increases to 10 % (Fig. S1, Table S1). Because changes in land use can happen very quickly compared to the time scale of updates in the model (10 years) the changes in sediment for RAI and RAII were incorporated at the beginning of the simulations. The RA III scenario included projection for increases in rainfall intensity under future climate change conditions,

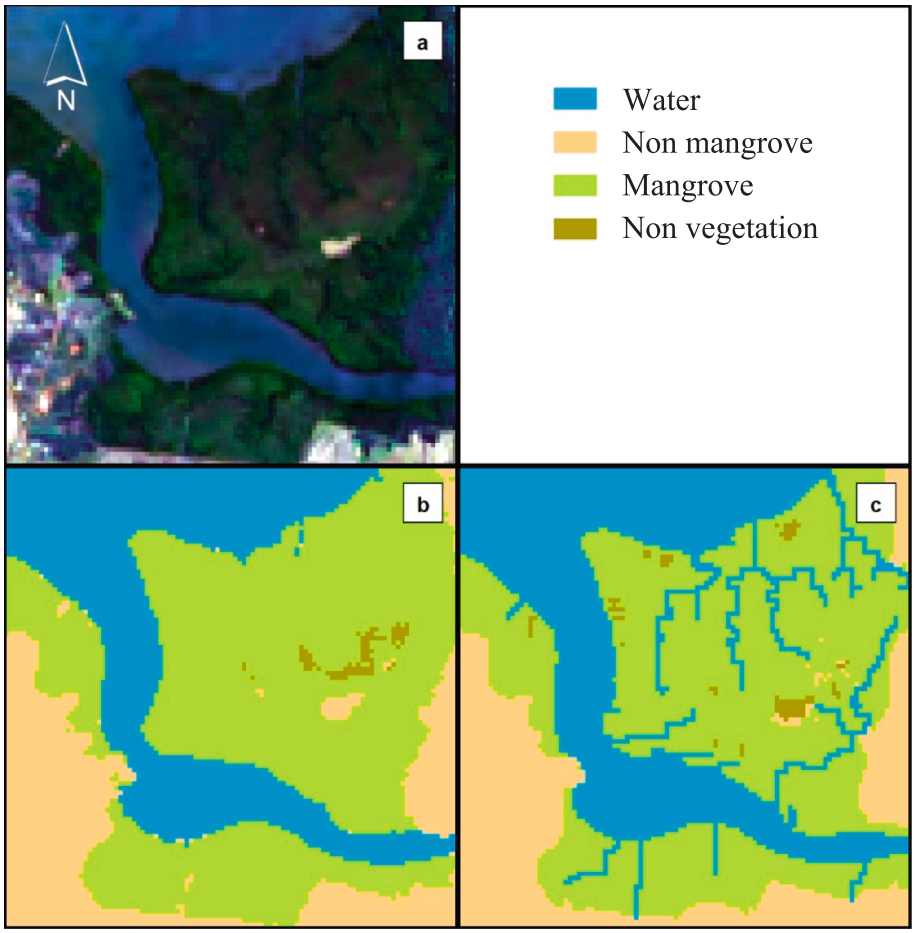


**Fig. 3.** Model evaluation using current mangrove distribution a) Landsat 8 image 22 May 2019, b) mangrove supervised classification, c) simulated mangrove areas.

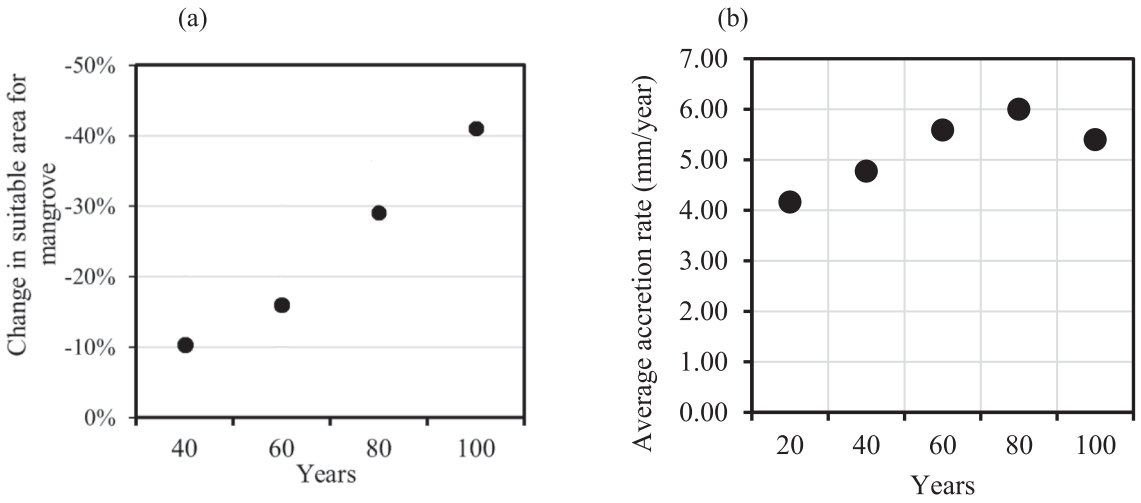


**Fig. 4.** Effect of SLR in baseline scenario: a) change in suitable area for mangroves with sea-level rise relative to the current area, and b) annual accretion rate of suitable area.

which resulted in sediment concentration increasing gradually over time from 0 to 60 % (from 40 mg/L to 64 mg/L) at the end of the 100-year period of simulation. This scenario considered an increase in temperature of 4 °C and an increase in precipitation intensity of extreme events of about 30 % (IPCC, 2021; Seneviratne et al., 2021) (Text S3). Finally, RA IV considered a 30 % reduction of sediment concentration. The objective of this simulation was to assess the system response to a potential reduction of the sediment supply, which can result from conservation practices (conversion from agriculture to natural vegetation) or from ad-hoc measures to prevent sediment reaching the coastal area. The simulation period for all scenarios was from 2020 to 2120 with a coupling time of 10 yrs i.e. the time period in which feedbacks from vegetation and accretion are redefined in the hydrodynamic model.

## 3. Results

### 3.1. Model verification

Due to the limited availability of on-the-ground data, the eco-geomorphological model could not be formally calibrated and validated as we have done in the past with other systems (Rodriguez et al., 2017; Sandi et al., 2018). Our approach consisted in setting up the model using the available information (including estimated sediment load and parameters obtained for similar systems) and verifying model results for current conditions in terms of observed vegetation distribution and accretion rates. These two sets of model results synthetise vegetation and geomorphological processes that are at the core of our modelling framework.

The vegetation distribution is the result of wetland topography, inundation regime provided by the hydrodynamic model, and vegetation preference to hydroperiod H and depth below mean high tide D. A good agreement between model results and observations of vegetation distribution gives confidence regarding the reconstruction of the topography from the ASTER GDEM adjusted for vegetation offset using Landsat images, the hydrodynamic model results, and the thresholds of H and D selected for the mangrove species of the wetland.

Under current conditions (year 2020 with 40 mg/L sediment concentration and initial topography), the model correctly predicted the spatial distribution of areas suitable for mangrove habitat. Fig. 3 shows the distribution of the vegetation obtained from satellite image (Fig. 3a and b) and from the model results based on conditions suitable for mangroves (Fig. 3c). The simulated areas with suitable conditions for mangroves capture the current extent of the mangrove vegetation. To identify areas of mangroves, we used Landsat 8–9 OLI/TIRS C2 L2 from 2018 to 2022 as Landsat has the same resolution as the SRTM used for developing the DEM and the cell resolution in the model. We selected a Landsat scene acquired on the 22 of May 2019 as this was the one with lower cloud cover (Fig. 3a). We then clipped the scene to the extent of our domain and created a True Colour Composite using Bands 4, 3 and 2 (red, green and blue). A supervised classification was performed on ArcGIS to separate mangrove, non-mangrove, water and non-vegetated areas. This classification was then visually assessed by comparing against the spectral signals using a False Colour Composite from bands 5, 4, and 3 (infrared, red, green) and a True Colour Composite 5, 6 and 7 (infrared, midinfrared1, midinfrared2). Once the extent of the vegetation was determined (Fig. 3b), the simulation of current mangrove conditions (Fig. 3c) was evaluated by using a confusion matrix and calculating of the overall accuracy and Cohen's κ. Overall accuracy from the confusion matrix was 0.89 and Cohen's κ was 0.83. This level of accuracy is remarkably good for predictive models of vegetation distribution (Sandi et al., 2021; Sahana et al., 2022). The areal extent of the mangrove wetland is 4.55 $km^2$ and estimated above-ground biomass for the current distribution of mangroves obtained from the model (Eq. (4)) was 335 t/Ha, which is within the expected range for the species in the area (Duke et al., 2012, 2013; Fatoyinbo et al., 2018; Komiyama et al., 2008).

In order to check the sensitivity of the model results to potential uncertainties in the DEM data, the entire topography was lowered and raised by 10 cm and the current conditions were simulated again. For practical purposes, these changes were implemented by increasing (SL+) or decreasing (SL−) the initial sea level by 10 cm. In both situations the model results did not match the observations, with the simulated mangrove coverage underpredicting the observed coverage by 15 % and 20 % for SL+ and SL−, respectively (See Text S4, Figs. S8 and S9). These changes in the DEM resulted in higher H values in SL+ and low D values in SL− leading to the underpredictions.

The other component of the model results that we tested was the prediction of accretion. Computation of accretion in our model (Eq. (3)) is based on D (from the hydrodynamic model) biomass B (from Eq. (4)) fitted to measurements with similar vegetation in the region as a function of D) sediment concentration C (from the catchment hydro sedimentological model) and sedimentation and trapping parameters for similar vegetation and sediment characteristics in the region. For the conditions corresponding to the first step in our accretion computations the model produced an average accretion value over all points in the domain covered by mangrove of 4.16 mm/yr (Fig. 4). There are no available records of measured accretion in mangroves in Fiji or neighboring islands, but Ellison (2010) estimated current values of accretion

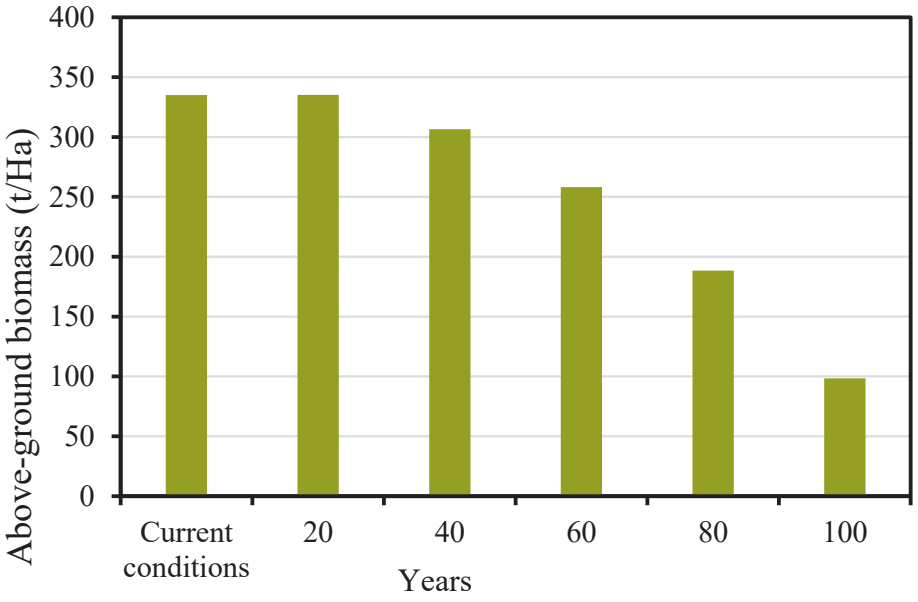


**Fig. 5.** Average mangrove above-ground biomass for the entire wetland over the simulation period for baseline scenario.

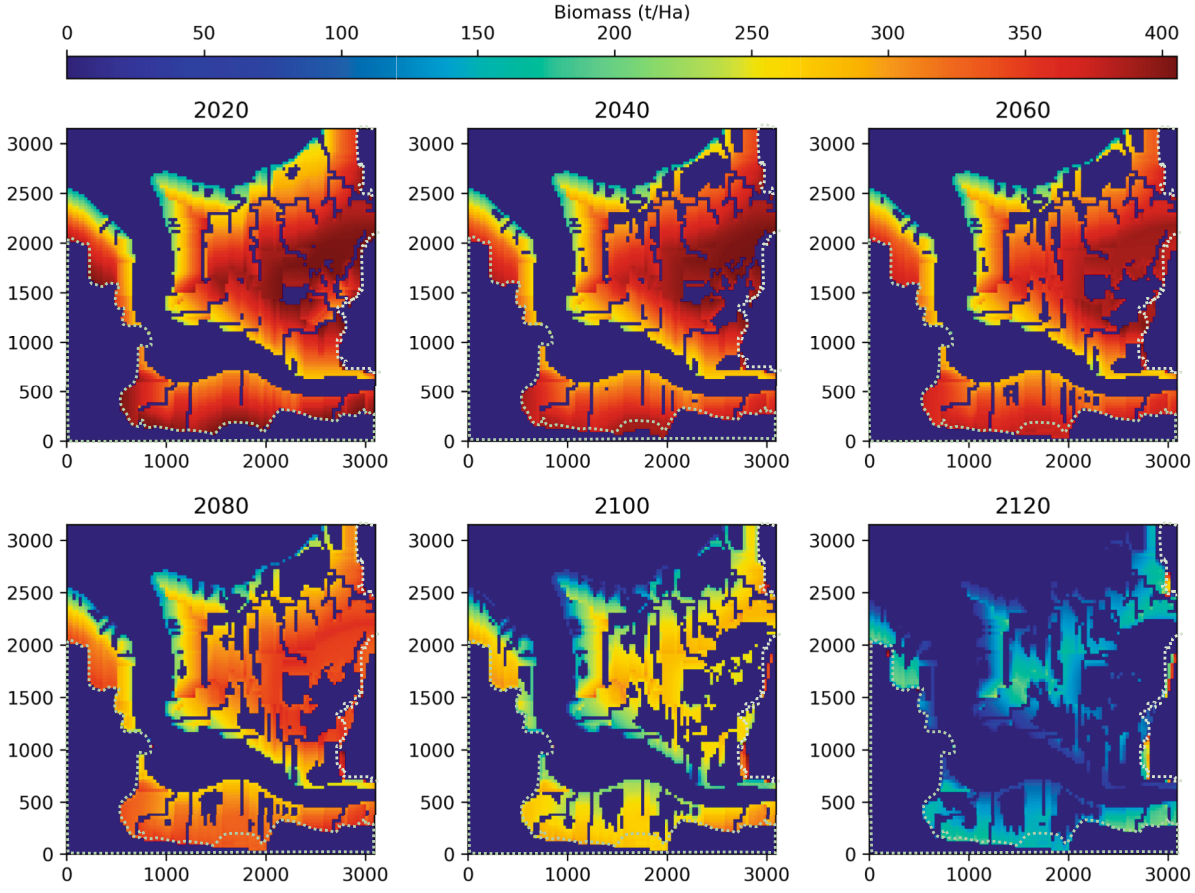


**Fig. 6.** Spatial distribution of mangrove above-ground biomass over the simulation period for baseline scenario. Dotted white line represents the initial boundary between mangrove and other vegetation.

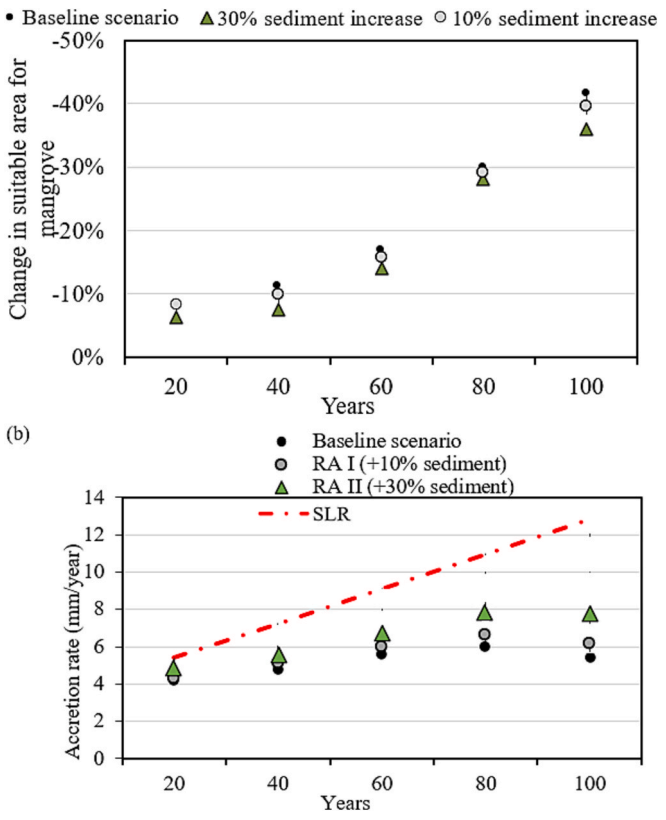


**Fig. 7.** Land use change effects (increase in sediment supply): a) change in suitable area for mangroves under land use change scenarios, b) SLR and accretion rates over time for different land use scenarios.

in high islands of Fiji (those that have fluvial sediment coming off the land into intertidal areas) at 4.5 mm/year based on stratigraphic reconstruction by Ellison and Stoddart (1991). This accretion value is very close to our model predictions and confirms the suitability of our setup, parameterisation, and data.

### 3.2. Resilience analysis under future climate change scenarios

#### 3.2.1. Sea level rise (Baseline)

The effects of SLR were evaluated over a period of 100 years. The rate of SLR used in our model corresponds to SSP5-8.5, with a 7.7 mm rise per year on average (IPCC, 2021). Fig. 4a shows the change in suitable area for mangroves under SLR conditions. During the first 40 years, the retreat of the mangroves is, on average, 5 % every 20 years; after that point, the rate of mangrove loss is accelerated, doubling this value. Fig. 4a also shows that after 100 years, the expected reduction of the wetland is over 40 %. This can be explained by the accretion rate, which, on average, is 5.5 mm/year (Fig. 4b), smaller than SLR (7.7 mm/year). The accretion rates of our model results agree with predictions for Indo-Pacific mangroves (Krauss et al., 2014; Lovelock et al., 2015; Elison, 2000).

It is important to observe not only the extension of the wetland, but also the condition of its forest health as indicated by the above-ground biomass (Doughty et al., 2021). Fig. 5 presents the temporal evolution, on average over the entire wetland, of the above-ground biomass. At the end of the simulation period, the above-ground biomass has reduced to a third of the initial conditions. This is due to reduction of the area suitable for mangroves and also because of the reduced biomass of the remaining trees (Fig. 6).

#### 3.2.2. Land use change scenarios (RA I and RA II)

The resilience analysis scenarios I and II (RA I and RA II) present an increment of sediment input to the wetland by 10 % and 30 %, respectively, due to changes in land use and land cover. Fig. 7 compares the RA I and RA II scenarios with current conditions. It shows that regardless of the increase in sediment supply, a significant proportion of the wetland will be lost by the beginning of next century (Fig. 7a). Even though there is an increase on the average accretion rates under the land-use change scenarios, it is not enough to keep up with the SLR rate (Fig. 7b).

After 100 years of simulations, the mangrove area reduction was 41.5 % for the baseline scenario and 39.6 % and 36.1 % for RA I and RA II, respectively. Although the area reduction was high in all the scenarios, Fig. 8 compares the biomass, highlighting that the state of the mangroves with more sediment supply was better than in the baseline scenario.

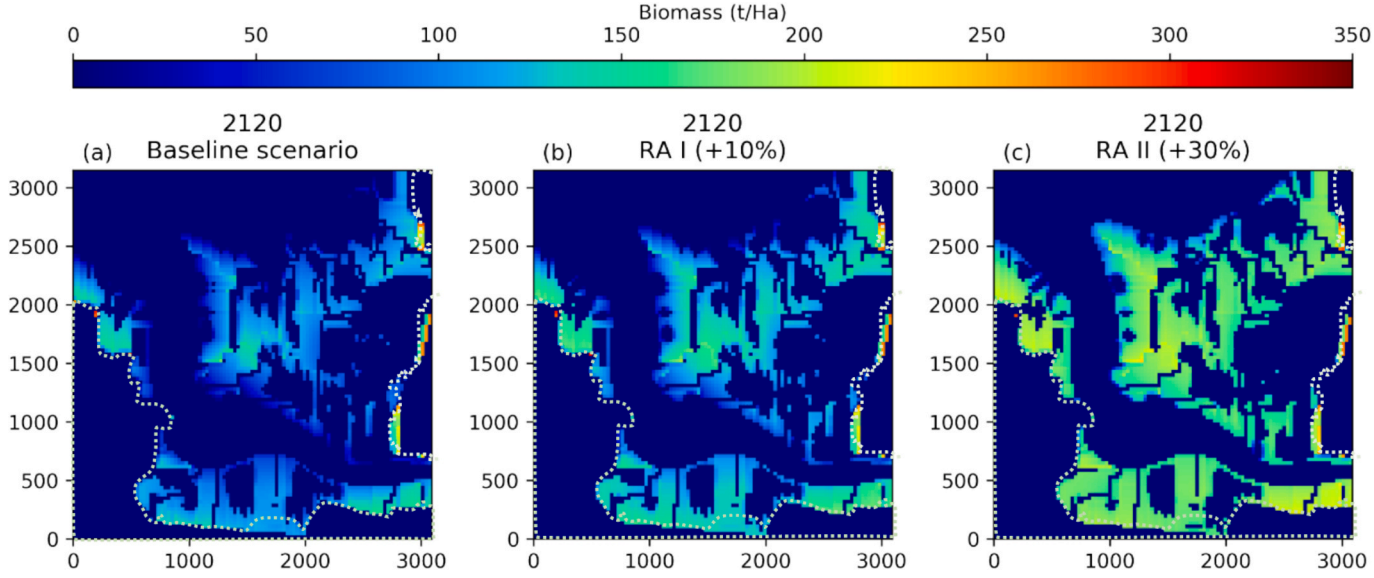


**Fig. 8.** Mangrove biomass comparison at the end of the simulation period for a) Baseline, b) RA I (10% increase in sediment) and, c) RA II scenarios (30% increase in sediment). Dotted white line represents the initial boundary between mangrove and other vegetation.

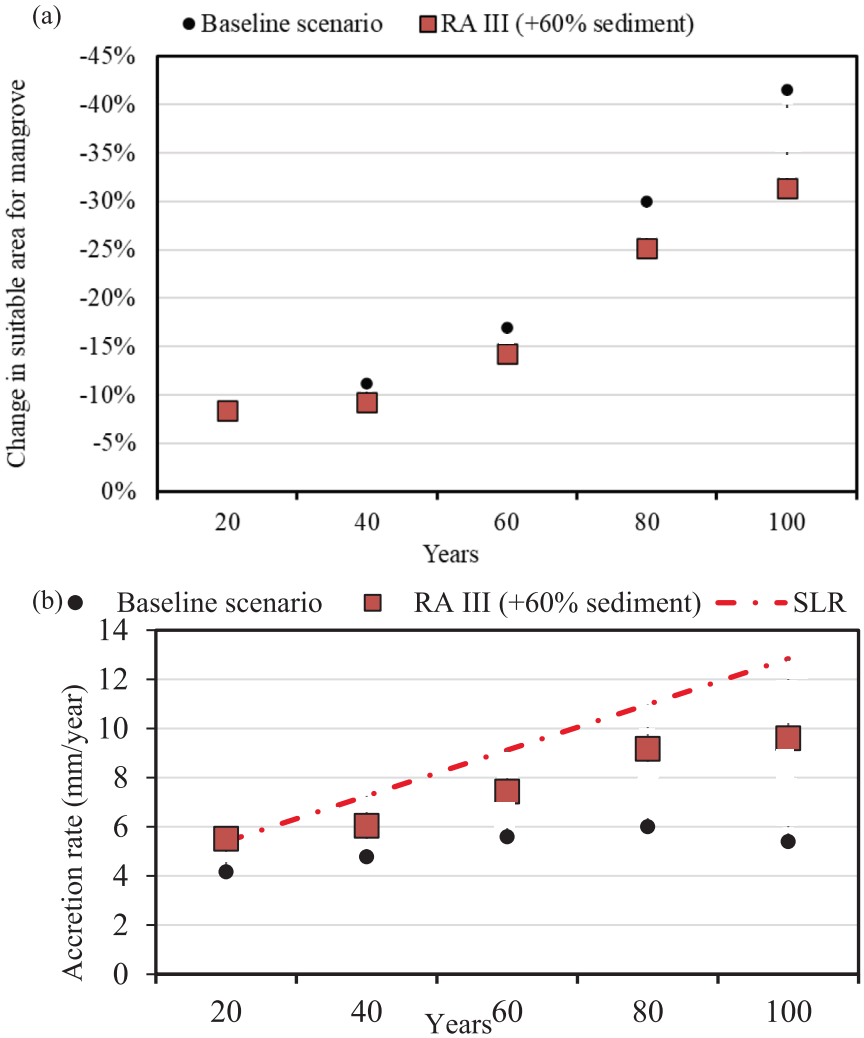


**Fig. 9.** Effects of climate change: a) change in suitable area for mangroves for the baseline and RAIII scenarios, b) SLR and accretion rates over time for the baseline and RA III scenarios.

*3.2.3. Climate change (RA III)*

The RA III scenario considered a gradual increase over the simulation period in the sediment supply from 0 to 60 %. The reduction of the area suitable for mangroves at the end of the simulation period was more than 30 % of the initial area, lower than in the baseline scenario (41.5 %), (Fig. 9a). Even though the sediment supply increased considerably over the latest part of the simulations, the wetland could not follow the SLR trend (Fig. 9b) and the biomass of the remaining mangroves was reduced to about half of the original value (Fig. 10).

*3.2.4. Reduction of the sediment inputs (RA IV)*

To assess the sensitivity of the wetland to reductions in sediment supply, a scenario with a reduction of 30 % of the baseline sediment concentrations was implemented. Fig. 11a shows the reduction of the area suitable for mangroves over time, in which the rate of area depletion was greater under a shortage of sediment supply than for any of the other scenarios due to the lower accretion capacity (Fig. 11b).

## 4. Discussion

The eco-geomorphological modelling implemented to the coastal mangrove wetland at the mouth of the Dreketi River captured the current distribution of the vegetation (Fig. 3), an above-ground biomass consistent with the expected ranges for the mangrove species present in the area (Duke et al., 2013; Fatoyinbo et al., 2018; Komiyama et al., 2008), and accretion rates for current conditions that agree with previous estimates for Fiji (Ellison, 2010).

A comparison among all the scenarios simulated is presented in Fig. 12, where a strong relation between sediment concentration and both the mangrove area and its elevation can be observed. The baseline situation, which considers that sediment inputs will remain unchanged in the future, results in average bio-geomorphic accretion rates (5.5 mm/year) substantially lower than the rate of sea-level rise (7.7 mm/year) and about 40 % of mangrove area losses by 2120. While there are no previous studies for this area that consider the temporal and spatial evolution of mangroves and the gradual area reduction, overall estimates of mangrove resilience based on current bio-geomorphic accretion rates and SLR levels similar to the ones used by us predict considerable stress on mangroves after 2060 (Ellison, 2010) and total submergence shortly after 2100 (Lovelock et al., 2015, Fig. 5c), which broadly agree with our predictions.

Even though the scenarios with high sediment loads conserve more mangrove suitable areas, all scenarios display considerable losses (between 30 % and 55 %) (Fig. 12a). Figs. 6, 8 and 10 indicate that the reduction in area is associated with a retreat of mangroves into higher ground, with almost no colonisation of new areas. The lack of buffer zones for colonisation in this wetland is due to the steep topography on the east and west boundaries of the mangrove area (Fig. 3) and a

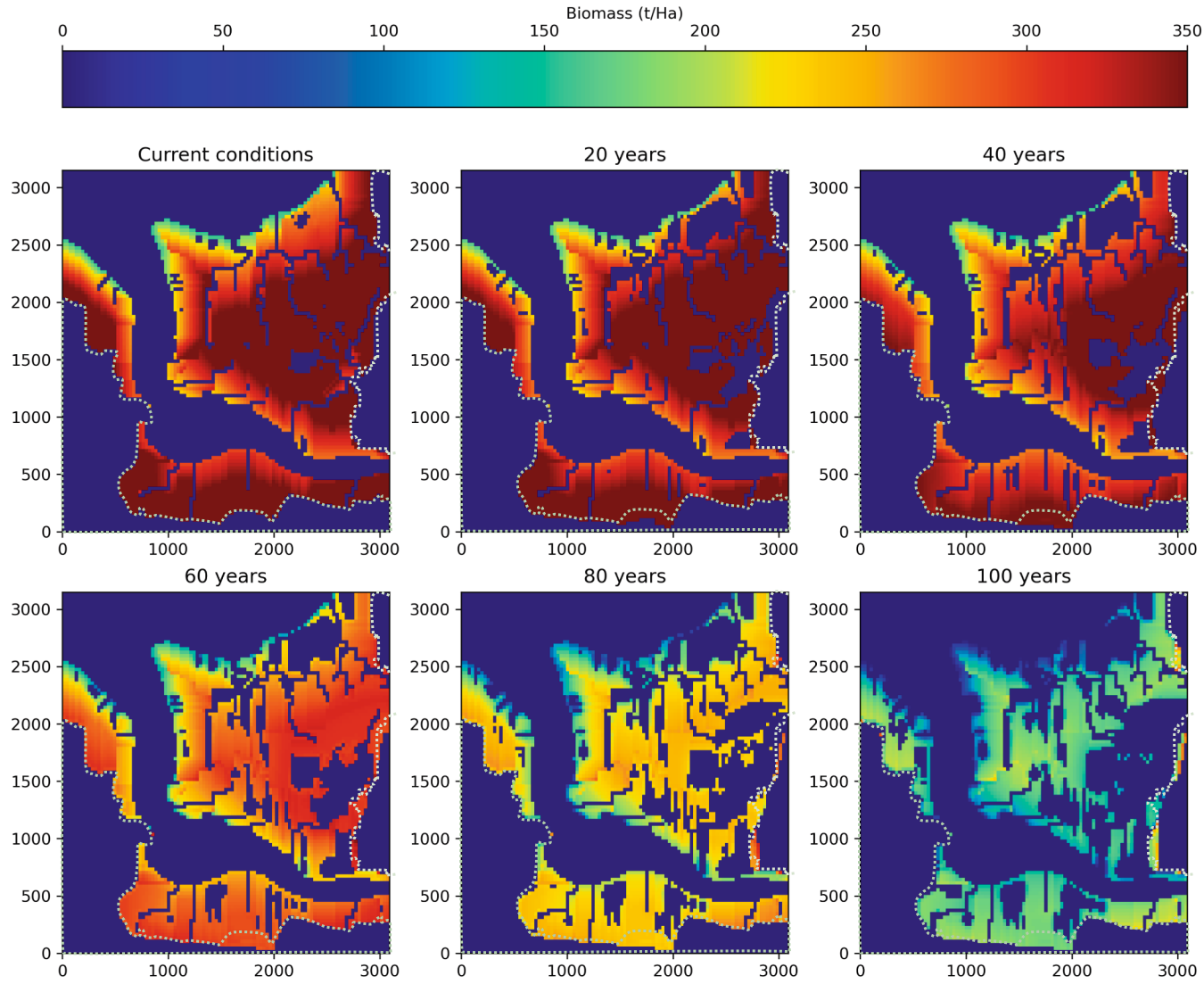


**Fig. 10.** Spatial distribution of mangrove above-ground biomass over the simulation period for RA III scenario. Dotted white line represents the initial boundary between mangrove and other vegetation.

manmade embankment on the south side.

The bio-geomorphic accretion in addition to the migration of mangroves to higher ground (limited by the surrounding topography) generates higher elevations in the remaining mangrove suitable area, as seen in Fig. 12b. The figure shows a strong positive influence of sediment supply on the changes in elevation of the mangrove suitable areas. When those elevations are compared with the sea level (also included in Fig. 12b) it can be seen that the wetland evolves from a situation where most of the mangrove areas are slightly above mean sea level (20–30 cm) to a situation in which they are at or below mean sea level. That lower position in the tidal frame is not favourable for mangrove establishment, a condition that is successfully captured by the eco-geomorphological model.

Another result from the simulations is that the system responds differently to increases and decreases in sediment concentration. Fig. 13 compares the suitable areas of the baseline scenario with the areas of two scenarios with a shift in sediment supply of + and − 30 %. In terms of suitable area, the negative effect of a 30 % reduction in sediment supply is more pronounced that the positive effect of a 30 % increase in sediment supply. This difference in behaviour is not reflected in the changes in elevation of Fig. 12b, where reductions or increases in sediment supply have the same proportional effects. So, even though the elevation changes of Fig. 12b may not be substantially lower with very low values of sediment supply, the extent of the wetland is considerably reduced. This is also shown by the biomass distributions of Fig. 14, which presents results at two stages of the simulation (2060 and 2120) for a reduction and an increase of the sediment supply. Reduction in sediment supply results in very low values of biomass, so a large portion of the increase in elevation is due to minerological deposition (see Eq. (2)).

Despite the fact that the effects of sediment supply on wetland accretion are widely covered in the literature on wetland evolution (Lovelock et al., 2015; D'Alpaos et al., 2007; Kirwan et al., 2010; Rodriguez et al., 2017) simulations are often carried out using rough estimates of this important input variable due to limitations on data availability. Coupling of a hydrosedimentological catchment model with the ecogeomorphological wetland model allows for a more integral and realistic analysis of the effects of sediment on wetland evolution. This coupling reveals, for example, that the effect of climate change on wetland evolution cannot be limited to SLR only, but it also has to consider potential increases in rainfall intensity (including cyclone activity in the case of the Pacific Islands) and temperature that can lead to substantial increases in sediment supply from the catchment. As Fig. 12 shows, expected increases in sediment due to climate change totally

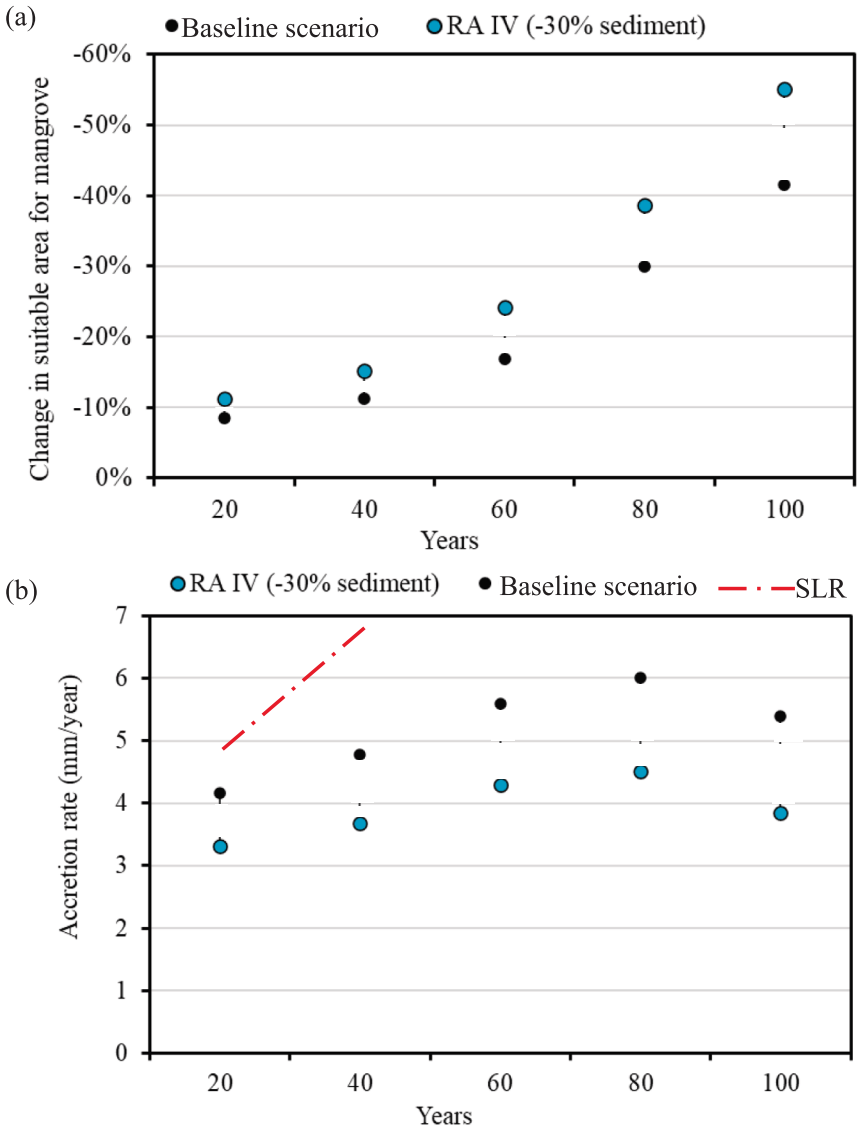


**Fig. 11.** Effects of a reduction of sediment supply: a) change in suitable area for mangroves under baseline scenario and a decrease in sediment supply, b) SLR and accretion rates under baseline scenario and a decrease in sediment supply.

changes the projections of wetland evolution and notably increases its resilience, delaying submergence by about 20 years. Even if the results for the Dreketi catchment could be considered to be at the high end of the spectrum compared to most of the world, they are certainly within the values expected for the Pacific Islands, which are known to be some of the areas more strongly affected by climate change.

The coupling of the two models also allows for the assessment of human interventions (land use changes due to agriculture, deforestation, etc) at the catchment scale, which is a prevalent issue on coastal catchments in the Pacific Islands and many other areas of the world. The magnitude of those effects are not as important in the Dreketi wetland due to limited availability of land that can potentially change use, but it can be more important in other sites, and particularly when combined with the effects of increased rainfall intensity due to climate change.

While this study provides valuable information regarding the potential fate of the study site under several scenarios of land use and climate change using advanced modelling tools, it has a number of limitations. The effect of large storms was incorporated through the sediment delivery from the catchment, which is an annual average value, but other effects like storm surge and episodic increases in sediment where not considered. This is consistent with the time scale of the simulations and supported by Rogers et al. (2013), which reported no noticeable change in the accretion trajectory of a wetland after a significant storm event. However, with increasing severity of storms projected as a result of climate change, extremely severe episodes may lead to complete collapse of the vegetation and transition to mudflats (Osland et al., 2020).

The scenarios of land use change that considered the increase in agricultural catchment areas resulted in higher values of sediment, which increased the accretion capacity and strengthened the opportunities for survival under SLR (Kirwan et al., 2010). However, this assessment does not consider other water quality aspects besides sediment, which may be important because runoff from agricultural areas may contain fertiliser or other pollutants that can affect the mangroves' health (Mack et al., 2024).

The reduced availability of field data was also a limitation in terms of model setup and parameterisation. Using SRTM as the basis for the model setup has unavoidable uncertainties, despite the checks and verifications carried out in this work. Lidar products can notably increase accuracy of DEMs and are a viable alternative in remote areas that can be readily incorporated in the framework presented in this contribution. In addition to this, many parameters of the models were based in

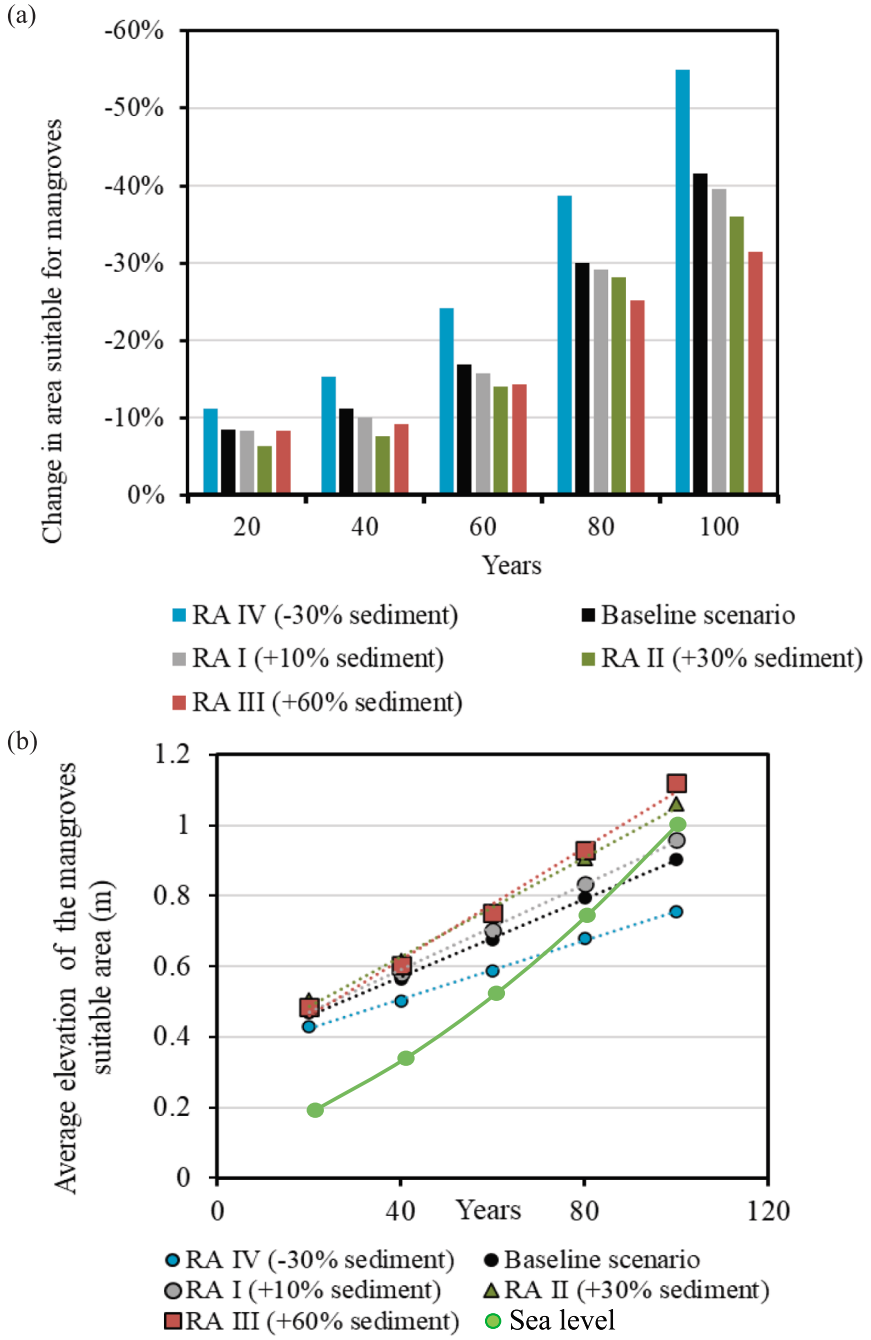


**Fig. 12.** Scenarios comparison: a) change in area suitable for mangrove, b) average elevation of the mangrove wetland over time.

regional studies or nearby sites, or on general charcteristics of soils and vegetation. Targeted field campaigns can provide valuable information on critical aspects like accretion rates, sediment properties, mangrove species distribution and biomass. Despite this limitations, the results of the model show strong trends driven by sea-level rise and sediment availability that are consistent with previous work.

The management implications of our results consist of two main aspects. The first one is to avoid any catchment measure that could restrict the sediment inputs to the mangrove forest, as that will limit the capacity of the wetland to accrete and compensate for some of the effects of sea-level rise. The other potential measure that could reduce vulnerability is the provision of buffer zones for mangrove migration. Those areas are currently restricted by an embankment and a drainaje chanel at the south end of the wetland, so a further analysis of these areas and the potential effects of removing those restrictions could be considered.

## 5. Conclusions

Due to the limited availability of field data at the study site, the proposed methodological approach relies heavily in remote sensing data and regional information. Verification of the model results were carried out indicating that the model correctly predicts the current distribution of the vegetation, the mangrove above-ground biomass and the accretion rates.

Future scenarios obtained using a hydro-sedimentological model on

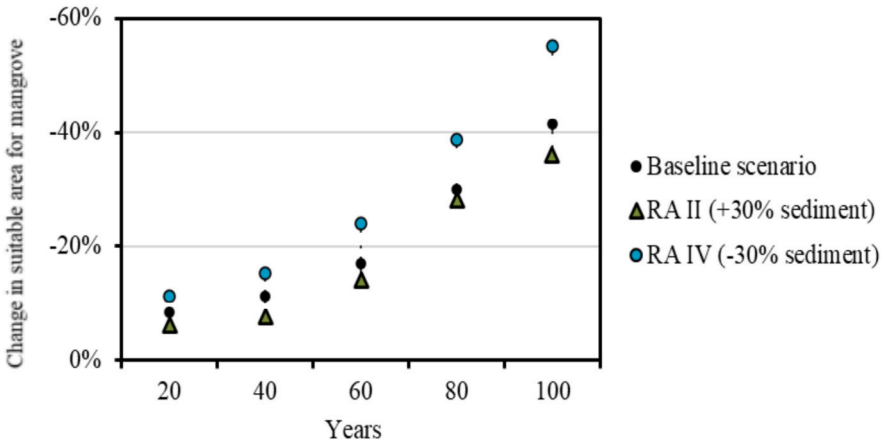


**Fig. 13.** Change in suitable area for mangroves for the baseline, RA II, and IV scenarios.

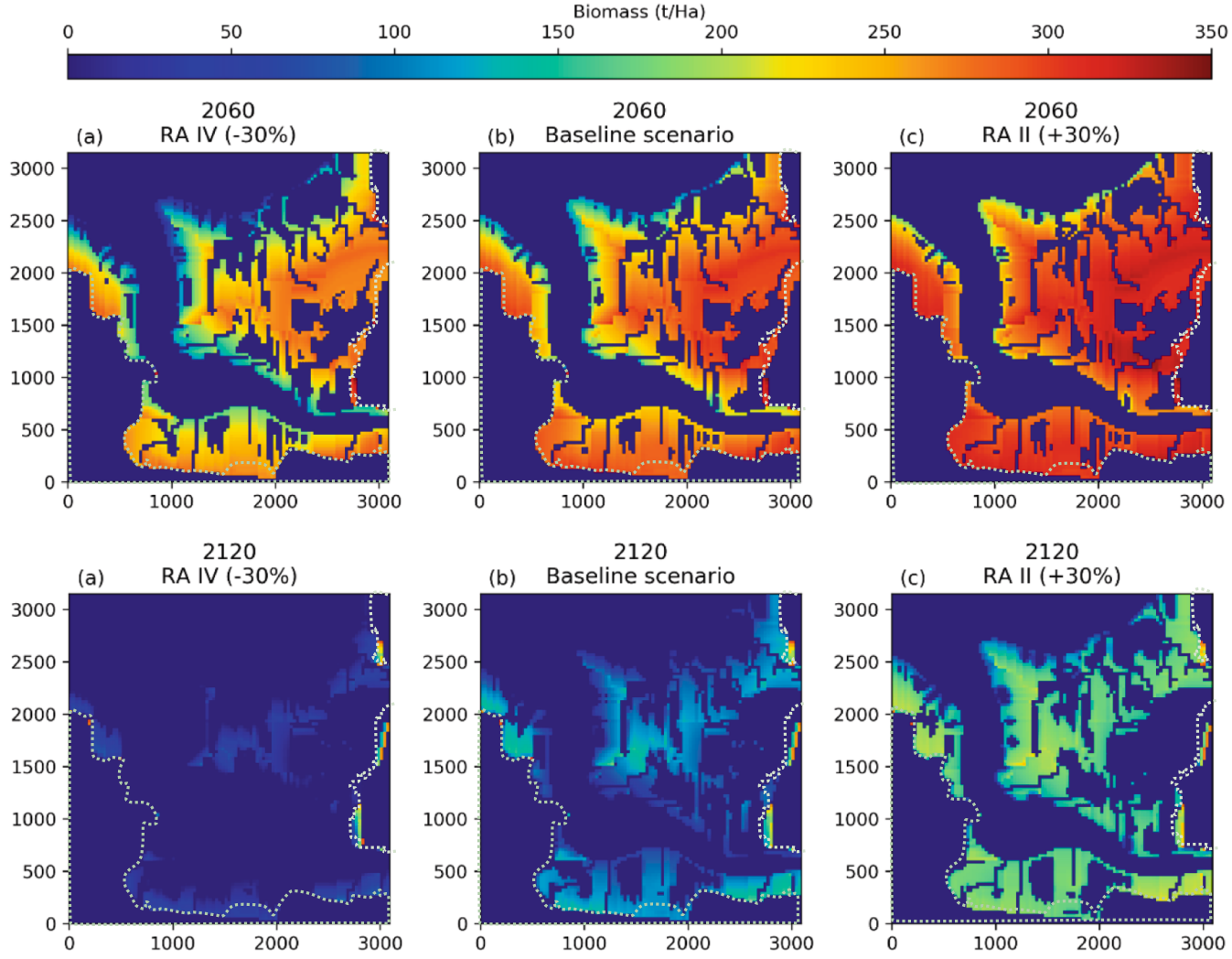


**Fig. 14.** Mangrove biomass distribution after 40 and 100 years of simulation for a) RA IV, b) baseline, and c) RA II scenarios. Dotted white line represents the initial boundary between mangrove and other vegetation.

the contributing catchment revealed that potential land use changes and increases in rainfall intensity due to climate change will result in an increase in sediment supply to the wetland compared to current conditions. The effects of these future changes combined with a SLR corresponding to SSP5-8.5 emissions path indicated more than 35 % of wetland loss over 100 years. The scenario that considered increases in rainfall intensity was the one with less wetland losses.

A strong relation between sediment inputs and the ability to the wetland to keep up with SLR was observed. However, the accretion rates obtained with the model were not enough to keep up with SLR. To test the model validity, a scenario with a decrease in sediment inputs with respect to current conditions was included, which resulted in massive losses of wetland area when combined with SLR.

The implementation of a distributed 2D eco-geomorphological model allowed for estimations of the extent of the mangrove coverage and its biomass distribution. Those estimates show that scenarios with greater sediment concentration resulted in higher mangrove biomass, which led to higher accretion rates and hence higher chances of survival. They also indicated that due to the topographic configuration of the wetland and a manmade embankment, its migration capacity is severely restricted and the only mechanism of the wetland to cope with sea-level rise is through vertical accretion.

## CRediT authorship contribution statement

**Eliana Jorquera:** Writing – original draft, Visualization, Validation, Software, Investigation, Formal analysis. **José F. Rodríguez:** Writing – review & editing, Supervision, Project administration, Methodology, Investigation, Conceptualization. **Patricia M. Saco:** Writing – review & editing, Supervision, Formal analysis, Conceptualization. **Steven Sandi:** Writing – review & editing, Investigation, Formal analysis. **Juan Quijano-Baron:** Writing – review & editing, Software, Investigation. **Angelo Breda:** Software, Methodology, Data curation.

## Declaration of competing interest

The authors declare that they have no known competing financial interests or personal relationships that could have appeared to influence the work reported in this paper.

## Acknowledgements

This research was funded by the University of Newcastle Postgraduate Research Scholarship (UNRSC) (E.J.).

## Appendix A. Supplementary material

Supplementary data to this article can be found online at https://doi.org/10.1016/j.catena.2025.109559.

## Data availability

Data will be made available on request.

## References

Ash, J. (1992). Vegetation ecology of Fiji: past, present, and future perspectives.

Beck, M.W., Heck, K.L., Able, K.W., Childers, D.L., Eggleston, D.B., Gillanders, B.M., Halpern, B., Hays, C.G., Hoshino, K., Minello, T.J., Orth, R.J., Sheridan, P.F., Weinstein, M.P., 2001. The identification, conservation, and management of estuarine and marine nurseries for fish and invertebrates: a better understanding of the habitats that serve as nurseries for marine species and the factors that create site-specific variability in nursery quality will improve conservation and management of these areas. Bioscience 51 (8), 633–641. https://doi.org/10.1641/0006-3568(2001)051[0633:Ticamo]2.0.Co;2.

Breda, A., Saco, P.M., Sandi, S.G., Saintilan, N., Riccardi, G., Rodríguez, J.F., 2021. Accretion, retreat and transgression of coastal wetlands experiencing sea-level rise. Hydrol. Earth Syst. Sci. 25 (2), 769–786. https://doi.org/10.5194/hess-25-769-2021.

Breda, A., Saco, P.M., Rodriguez, J.F., Sandi, S.G., Riccardi, G., 2022. Assessing the effects of sediment and tidal level variability on coastal wetland evolution. J. Hydrol. 613. https://doi.org/10.1016/j.jhydrol.2022.128387.

Brown, C.J., Jupiter, S.D., Albert, S., Klein, C.J., Mangubhai, S., Maina, J.M., Mumby, P., Olley, J., Stewart-Koster, B., Tulloch, V., Wenger, A., 2017. Tracing the influence of land-use change on water quality and coral reefs using a Bayesian model. Scientific Reports 7, 4740.

Cahoon, D.R., McKee, K.L., Morris, J.T., 2021. How plants influence resilience of salt marsh and mangrove wetlands to sea-level rise. Estuar. Coasts 44, 883–898. https://doi.org/10.1007/s12237-020-00834-w.

Cherry, J.A., Battaglia, L.L., 2019. Tidal wetlands in a changing climate: introduction to a special feature. Wetlands 39, 1139–1144. https://doi.org/10.1007/s13157-019-01245-9.

Crase, B., Liedloff, A., Vesk, P.A., Burgman, M.A., Wintle, B.A., 2013. Hydroperiod is the main driver of the spatial pattern of dominance in mangrove communities. Glob. Ecol. Biogeogr. 22 (7), 806–817. https://doi.org/10.1111/geb.12063.

D'Alpaos, A., Lanzoni, S., Marani, M., Rinaldo, A., 2007. Landscape evolution in tidal embayments: modeling the interplay of erosion, sedimentation, and vegetation dynamics. J. Geophys. Res. Earth 112 (F1). https://doi.org/10.1029/2006jf000537.

Dietrich, J.C., et al., 2011. Hurricane Gustav (2008) waves and storm surge: hindcast, synoptic analysis, and validation in Southern Louisiana. Mon. Weather Rev. 139, 2488–2521.

Doughty, C.L., Ambrose, R.F., Okin, G.S., Cavanaugh, K.C., 2021. Characterizing spatial variability in coastal wetland biomass across multiple scales using UAV and satellite imagery. Remote Sens. Ecol. Conserv. 7 (3), 411–429. https://doi.org/10.1002/rse2.198.

Duke, N. C., Mackenzie, J., & Wood, A. (2012). A revision of mangrove plants of the Solomon Islands, Vanuatu, Fiji, Tonga and Samoa (Centre for Tropical Water & Aquatic Ecosystem Research (TropWATER) Publication, Issue.

Duke, N. C., Mackenzie, J., & Wood, A. (2013). Preliminary assessment of biomass and carbon content of mangroves in Solomon Islands, Vanuatu, Fiji, Tonga and Samoa (Centre for Tropical Water & Aquatic Ecosystem Research (TropWATER) Publication, Issue.

Ellison, J.C., 2000. How south pacific mangroves may respond to predicted climate change and sea-level rise. In: Gillespie, A., Burns, W.C.G. (Eds.), Climate Change in the South Pacific: Impacts and Responses in Australia, New Zealand, and Small Island States. Advances in Global Change Research. Springer, Dordrecht. https://doi.org/10.1007/0-306-47981-8_16.

Ellison, J. C. (2010). Vulnerability of Fiji's mangroves and associated coral reefs to climate change. A Review. Suva, Fiji, WWF South Pacific Office.

Ellison, J.C., Stoddart, D.R., 1991. Mangrove ecosystem collapse during predicted sea-level rise: holocene analogues and implications. J. Coast. Res. 7 (1), 151–165.

Fagherazzi, S., Kirwan, M.L., Mudd, S.M., Guntenspergen, G.R., Temmerman, S., D'Alpaos, A., Van de Koppel, J., Rybczyk, J.M., Reyes, E., Craft, C., 2012. Numerical models of salt marsh evolution: Ecological, geomorphic, and climatic factors. Reviews of Geophysics 50.

Fatoyinbo, T., Feliciano, E.A., Lagomasino, D., Lee, S.K., Trettin, C., 2018. Estimating mangrove aboveground biomass from airborne LiDAR data: a case study from the Zambezi River delta. Environ. Res. Lett. 13 (2), 025012.

Feher, L.C., Osland, M.J., Anderson, G.H., et al., 2020. The long-term effects of hurricanes Wilma and Irma on soil elevation change in everglades mangrove forests. Ecosystems 23, 917–931. https://doi.org/10.1007/s10021-019-00446-x.

Hayden, H.L., Granek, E.F., 2015. Coastal sediment elevation change following anthropogenic mangrove clearing. Estuar. Coast. Shelf Sci. 165, 70–74. https://doi.org/10.1016/j.ecss.2015.09.004.

Intergovernmental Panel on Climate Change. (2021). Climate change 2021: the physical science basis. contribution of working group I to the sixth assessment report of the intergovernmental panel on climate change (Vol. In Press). Cambridge University Press. https://doi.org/10.1017/9781009157896.

Jorquera, E., Saco, P.M., Verdon-Kidd, D., Rodríguez, J.F., Timmermans, H., Nelson, F., 2024. Effects of tropical cyclones on catchment sediment delivery to coastal ecosystems. Catena 238, 107805. https://doi.org/10.1016/j.catena.2024.107805.

Kauffman, J.B., Heider, C., Cole, T.G., Dwire, K.A., Donato, D.C., 2011. Ecosystem carbon stocks of Micronesian mangrove forests. Wetlands 31 (2), 343–352. https://doi.org/10.1007/s13157-011-0148-9.

Kelleway, J.J., Cavanaugh, K., Rogers, K., Feller, I.C., Ens, E., Doughty, C., Saintilan, N., 2017. Review of the ecosystem service implications of mangrove encroachment into salt marshes. Glob. Chang. Biol. 23 (10), 3967–3983. https://doi.org/10.1111/gcb.13727.

Kirwan, M.L., Megonigal, J.P., 2013. Tidal wetland stability in the face of human impacts and sea-level rise. Nature 504 (7478), 53. https://www.nature.com/articles/nature12856.pdf.

Kirwan, M.L., Guntenspergen, G.R., D'Alpaos, A., Morris, J.T., Mudd, S.M., Temmerman, S., 2010. Limits on the adaptability of coastal marshes to rising sea level. Geophys. Res. Lett. 37 (23). https://doi.org/10.1029/2010GL045489.

Kirwan, M.L., Temmerman, S., Skeehan, E.E., Guntenspergen, G.R., Fagherazzi, S., 2016. Overestimation of marsh vulnerability to sea level rise. Nat. Clim. Chang. 6 (3), 253.

Knight, D., 1981. Some field measurements concerned with the behaviour of resistance coefficients in a tidal channel. Estuar. Coast. Shelf Sci. 12, 303–322.

Komiyama, A., Ong, J.E., Poungparn, S., 2008. Allometry, biomass, and productivity of mangrove forests: a review. Aquat. Bot. 89 (2), 128–137.

Kostaschuk, R.A.Y., Terry, J., Raj, R., 2001. Tropical cyclones and floods in Fiji. Hydrological Sciences Journal 46, 435–450.

Krauss, K.W., Lovelock, C.E., McKee, K.L., López-Hoffman, L., Ewe, S.M., Sousa, W.P., 2008. Environmental drivers in mangrove establishment and early development: a review. Aquat. Bot. 89 (2), 105–127.

Krauss, K.W., McKee, K.L., Lovelock, C.E., Cahoon, D.R., Saintilan, N., Reef, R., Chen, L., 2014. How mangrove forests adjust to rising sea level. New Phytol. 202 (1), 19–34. https://nph.onlinelibrary.wiley.com/doi/pdf/10.1111/nph.12605.

Lovelock, C.E., Cahoon, D.R., Friess, D.A., Guntenspergen, G.R., Krauss, K.W., Reef, R., Rogers, K., Saunders, M.L., Sidik, F., Swales, A., 2015. The vulnerability of Indo-Pacific mangrove forests to sea-level rise. Nature 526 (7574), 559. https://www.nature.com/articles/nature15538.pdf.

Ludwig, C., Walli, A., Schleicher, C., Weichselbaum, J., Riffler, M., 2019. A highly automated algorithm for wetland detection using multi-temporal optical satellite data. Remote Sens. Environ. 224, 333–351. https://doi.org/10.1016/j.rse.2019.01.017.

Mack, M.R., Langley, J.A., Feller, I.C., Chapman, S.K., 2024. The ecological consequences of nutrient enrichment in mangroves. Estuar. Coast. Shelf Sci. 300, 108690. https://doi.org/10.1016/j.ecss.2024.108690.

Magee, A.D., Verdon-Kidd, D.C., Kiem, A.S., Royle, S.A., 2016. Tropical cyclone perceptions, impacts and adaptation in the Southwest Pacific: An urban perspective from Fiji, Vanuatu and Tonga. Natural Hazards and Earth System Sciences 16, 1091–1105.

Mazda, Y., et al., 1997. Drag force due to vegetation in mangrove swamps. Mangroves Salt Marshes 1, 193–199.

McInnes, K.L., Walsh, K.J.E., Hoeke, R.K., O'Grady, J.G., Colberg, F., Hubbert, G.D., 2014. Quantifying storm tide risk in Fiji due to climate variability and change. Global and Planetary Change 116, 115–129.

Morris, J.T., Sundareshwar, P.V., Nietch, C.T., Kjerfve, B., Cahoon, D.R., 2002. Responses of coastal wetlands to rising sea level. Ecology 83 (10), 2869–2877. https://doi.org/10.1890/0012-9658(2002)083[2869:ROCWTR]2.0.CO;2.

Morris, J.T., Langley, J.A., Vervaeke, W.C., Dix, N., Feller, I.C., Marcum, P., Chapman, S. K., 2023. Mangrove trees outperform saltmarsh grasses in building elevation but collapse rapidly under high rates of sea-level rise. Earth's Future 11, e2022EF003202.

Osland, M.J., Feher, L.C., Anderson, G.H., et al., 2020. A tropical cyclone-induced ecological regime shift: mangrove forest conversion to mudflat in everglades National Park (Florida, USA). Wetlands 40, 1445–1458. https://doi.org/10.1007/s13157-020-01291-8.

Ramsar Convention, Secretariat., 2019. The list of wetlands of international importance. Ramsar Secretariat, Gland, Switzerland.

Riccardi, G., 2000. A cell model for hydrological-hydraulic modeling. J. Environ. Hydrol. 8, 15. http://www.hydroweb.com/jeh/jeh2000/riccardi.pdf.

Rodriguez, J.F., Saco, P.M., Sandi, S., Saintilan, N., Riccardi, G., 2017. Potential increase in coastal wetland vulnerability to sea-level rise suggested by considering hydrodynamic attenuation effects. Nat. Commun. 8, 16094. https://doi.org/10.1038/ncomms16094.

Rogers, K., Saintilan, N., Howe, A., Rodriguez, J.F., 2013. Sedimentation, elevation and marsh evolution in a southeastern Australian estuary during changing climatic conditions. Estuar. Coast. Shelf Sci. https://doi.org/10.1016/j.ecss.2013.08.025.

Saco, P.M., Rodríguez, J.F., 2013. Modeling ecogeomorphic systems. In: Shroder, J.F. (Ed.), *Treatise on Geomorphology*. Academic Press, pp. 201–220. https://doi.org/10.1016/B978-0-12-374739-6.00038-5.

Sahana, M., Areendran, G., Sajjad, H., 2022. Assessment of suitable habitat of mangrove species for prioritizing restoration in coastal ecosystem of Sundarban Biosphere Reserve, India. Sci. Rep. 12, 20997. https://doi.org/10.1038/s41598-022-24953-5.

Saintilan, N., Khan, N.S., Ashe, E., Kelleway, J.J., Rogers, K., et al., 2020. Thresholds of mangrove survival under rapid sea level. Science 368 (6495), 1118–1121.

Sandi, S.G., Rodríguez, J.F., Saintilan, N., Riccardi, G., Saco, P.M., 2018. Rising tides, rising gates: the complex ecogeomorphic response of coastal wetlands to sea-level rise and human interventions. Adv. Water Resour. 114, 135–148. https://doi.org/10.1016/j.advwatres.2018.02.006.

Sandi, S.G., Rodriguez, J.F., Saco, P.M., Saintilan, N., Riccardi, G., 2021. Accelerated sea-level rise limits vegetation capacity to sequester soil carbon in coastal wetlands: a study case in South-Eastern Australia. Earth's Future 9. https://doi.org/10.1029/2020ef001901.

Scott, D. A. (1993). A directory of wetlands in Oceania. IWRB.

Seneviratne, S.I., Zhang, X., Adnan, M., Badi, W., Dereczynski, C., Di Luca, A., Ghosh, S., Iskandar, I., Kossin, J., Lewis, S., Otto, F., Pinto, I., Satoh, M., Vicente-Serrano, S.M., Wehner, M., Zhou, B., 2021. Weather and climate extreme events in a changing climate. In: Masson-Delmotte, V., Zhai, P., Pirani, A., Connors, S.L., Péan, C., Berger, S., Caud, N., Chen, Y., Goldfarb, L., Gomis, M.I., Huang, M., Leitzell, K., Lonnoy, E., Matthews, J.B.R., Maycock, T.K., Waterfield, T., Yelekçi, O., Yu, R., Zhou, B. (Eds.), Climate change 2021: The physical science basis. Contribution of Working Group I to the Sixth Assessment Report of the Intergovernmental Panel on Climate Change. Cambridge University Press.

Smith, T.J., 1987. Effects of light and intertidal position on seedling survival and growth in tropical tidal forests. Journal of Experimental Marine Biology and Ecology 110, 133–146.

Secretariat of the Pacific Regional Environment Programme. (2016). State of conservation in Fiji: country report 2013.

Secretariat of the Pacific Regional Environment Programme. (2017). Ecosystem & Socio-economic Resilience Analysis & Mapping (ESRAM) for Macuata Province, Fiji. (Pacific Ecosystem-Based Adaption to Climate Change Project., Issue.

Terry, J.P., McGree, S., Raj, R., 2004. The exceptional flooding on Vanua Levu Island, Fiji, during Tropical Cyclone Ami in January 2003. Journal of Natural Disaster Science 26, 27–36.

van Maanen, B., Coco, G., Bryan, K.R., 2015. On the ecogeomorphological feedbacks that control tidal channel network evolution in a sandy mangrove setting. Proc. Royal Soc. A: Math., Phys. Eng. Sci. 471 (2180), 20150115. https://doi.org/10.1098/rspa.2015.0115.

Woodroffe, C.D., Rogers, K., McKee, K.L., Lovelock, C.E., Mendelssohn, I., Saintilan, N., 2016. Mangrove sedimentation and response to relative sea-level rise. Ann. Rev. Mar. Sci. 8, 243–266. https://www.annualreviews.org/doi/pdf/10.1146/annurev-marine-122414-034025.